Polym. Bull. (2012) 69:579–595
DOI 10.1007/s00289-012-0752-8

ORIGINAL PAPER

Thermo-sensitive polymers based on graft polysiloxanes

Anca Daniela Rusu Hodorog · Constanta Ibanescu · Maricel Danu · Bogdan C. Simionescu · Licinio Rocha · Nicolae Hurduc

Received: 27 September 2011 / Revised: 10 February 2012 / Accepted: 3 April 2012 /
Published online: 10 April 2012

Abstract The synthesis of novel polymers obtained by grafting poly(dimethyl siloxane) with NIPAM, *N,N′*-dimethyl acrylamide (DMA) and copolymers of NIPAM with DMA and butyl acrylate using SET-LRP technique is presented. The polymers were characterized by ^{1}H NMR, fluorescence spectroscopy, and DSC. The thermo-sensitivity and the LCST as well as the aggregation phenomena during phase transition are evidenced by dynamic light scattering (DLS) and rheology coupled with small angle light scattering (SALS). Rheological and Rheo-SALS measurements proved to be useful tools to characterize the macroscopic behavior but also to evidence structural changes below and above the LCST for the analyzed systems. Good correlation was found between rheological, rheo-SALS and DLS data.

Keywords Thermo-sensitive polymers · Polysiloxanes · Poly(*N*-isopropylacrylamide) · Rheo-SALS · Rheology

A. D. R. Hodorog · C. Ibanescu (✉) · B. C. Simionescu · N. Hurduc (✉)
Department of Natural and Synthetic Polymers, "Gheorghe Asachi" Technical University of Iasi, Prof. D. Mangeron Street 73, 700050 Iasi, Romania
e-mail: ibanescu@ch.tuiasi.ro

N. Hurduc
e-mail: nhurduc@ch.tuiasi.ro

C. Ibanescu · M. Danu · B. C. Simionescu
Petru Poni Institute of Macromolecular Chemistry, Ghica Voda Alley 41A, 700487 Iasi, Romania

L. Rocha
CEA, LIST Saclay, Laboratoire Capteurs et Architectures Électroniques, 91191 Gif-sur-Yvette Cedex, France

Introduction

Controlled drug delivery systems have gained a lot of interest in the scientific community offering the possibility to target the drug to a specific destination, and to monitor the delivering process overcoming the limitations of conventional drug formulations. Stimuli sensitive polymers are suited for many biomedical and biotechnological applications [1–11] being able to respond to external stimuli in a controlled manner. Among different types of physical or chemical external stimuli (temperature, electric or magnetic fields, mechanical stress, pH, ionic factors, and chemical agents) used to tune the structure and/or properties of polymeric systems, temperature is probably the most widely used [2, 7, 8, 11–15]. Thermo-sensitive polymers posses a set of unique properties and among them of outstanding importance is the existence of a critical solution temperature usually a lower critical solution temperature (LCST) [2, 11, 13–15]. Poly(*N*-isopropylacrylamide) (PNIPAM) was extensively studied and became probably the most popular thermo-sensitive polymer possessing a lower critical solution temperature (LCST) in water at around 31–32 °C [2, 14–17]. Above 32 °C PNIPAM exhibits a phase transition [17] and if below 30 °C the polymer is soluble in water with heating its solubility disappears due to conformational changes. The LCST may be tailored by means of different chemical methods using either the functionality of the backbone or the copolymerization strategies. For drug delivery and biological systems it is very important to bring LCST as close as possible to the physiological temperature that is around 37 °C. Coupling *N*-isopropylacrylamide (NIPAM) to polymers bearing hydrophilic and/or hydrophobic groups in their chain offers the opportunity to control the phase transition temperature and to tailor new materials with different architectures and tunable properties [11–18]. An alternative of combining PNIPAM with different polymers is to graft NIPAM on the macromolecular chain [6, 14]. However, to the best of our knowledge, references about the graft copolymerization of thermo-sensitive monomers such as NIPAM onto polysiloxanic chains could not be found in the literature. Hence further investigation on the synthesis, characterization and potential application of such polymers are needed.

Living radical polymerization (LRP) allows precise control of the polymers architecture, molecular weight, and molecular weight distribution proving to be an attractive technique for the synthesis of thermo-sensitive polymers with desirable properties [18–22]. Among various LRP methods, single-electron transfer living radical polymerization (SET-LRP) developed by Percec et al. [21] has become a useful and rapid tool for the synthesis of well-defined polymers with high control over molecular architecture and functionality [19–22]. SET-LRP using Cu(0) powder [23–28] or Cu(0) wire [29–34] in conjunction with a appropriate combination of ligand and solvent is a relative simple and versatile synthesis method suitable for a large combination of monomers [19]. The SET-LRP synthesis of water-soluble polymers with potential biological applications has been reported [22].

This study presents the synthesis and characterization of novel polymers obtained by grafting poly(dimethyl siloxane) (PDMS) with NIPAM, *N,N′*-dimethyl acrylamide (DMA) and copolymers of NIPAM with DMA and butyl acrylate (BA) using SET-LRP technique thus developing polymers characterized by high flexibility and

controlled thermo-sensitivity. More hydrophilic monomers such as acrylamide would make the LCST increase and even disappear, and more hydrophobic monomers such as BA would induce the LCST to decrease. In this way, the LCST could be controlled by incorporation of hydrophobic or hydrophilic moieties to adjust to a desired LCST. It is expected that the specific behavior of the obtained polymers to mainly derive from the particular architecture involving hydrophilic branches attached to a hydrophobic, flexible main-chain involving a coil to micelle transition. The balance between the hydrophilic and hydrophobic segments also influences the solution behavior of the obtained polymers. Effects of the side chains structure on the thermal and rheological properties were investigated. Owing to the anticipated properties the new systems can show potential for biological applications, especially as controlled drug delivery systems.

Experimental part

Materials

The monomer NIPAM (Aldrich) was recrystallized in *tert*-butanol and dried under vacuum prior to use in radical polymerization. Before the synthesis DMA (Aldrich) and BA (Merck) were passed once through a basic-alumina column to remove the polymerization inhibitor. 2,2′-bipyridyl (bipy) (Fluka) was purified by re-crystallization, dried under vacuum, and stored under argon. All other solvents (chloroform, dimethylsulfoxide (DMSO), diethyl ether) and chemicals were from Aldrich and used as received. The synthesis and purification of the macroinitiator (linear polysiloxane with chlorobenzyl side groups) (PSI) used in this study was performed according to the methodology previously described in [35].

Synthesis of graft polymers by SET-LRP

Linear polysiloxane containing chlorobenzyl groups in the side chain (PSI) was used as macroinitiator in the SET-LRP reaction. In a typical reaction 0.0915 g bipy were added to 0.1 g PSI previously dissolved in DMSO (1.5 mL). The mixture was introduced in a 25 mL flask where 1.5 g of the corresponding monomer/monomers (the amount of each monomer depending on the desired copolymerization ratios) and Cu wire (0.25 g) were added under stirring. The system was degassed by five freeze–pump–thaw cycles. The flask was heated at the reaction temperature (80 °C) and the synthesis was performed under nitrogen for 8 h (Scheme 1). At the end of the reaction, the polymerization mixture was diluted with $CHCl_3$ and the catalyst was removed by passing the solution through alumina. The clear solution was then precipitated in diethyl ether and dried under vacuum.

PNIPAM was synthesized by free radical polymerization. In a 25 mL flask 1 g NIPAM was dissolved in 2.07 mL of toluene and the benzoyl peroxide (BP) was added (0.034 g) under stirring. The reaction was performed for 3 h at 95 °C. At the end of the reaction the polymer was precipitated in diethyl ether, washed with

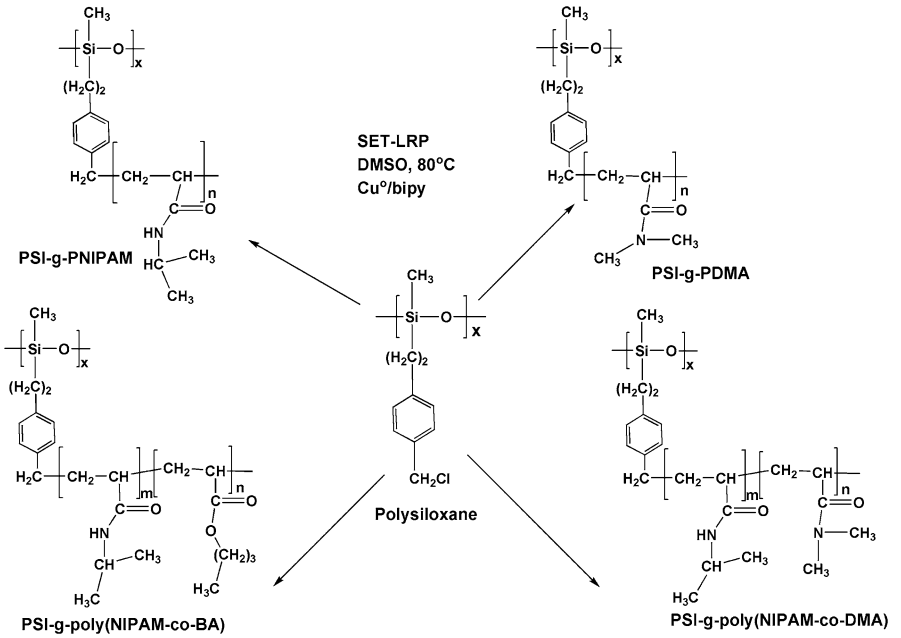

Scheme 1 Synthesis of graft polysiloxanes

Table 1 Characteristics of different graft polysiloxanes

Sample code	Sample	Chemical composition of the side chain	Grafting degree (%)	Molecular weight	LCST (°C)
D1	PNIPAM	–	–	36,000	31
D2	PSI–*g*–PNIPAM	NIPAM	87	60,000	31–32
D3	PSI–*g*–PDMA	DMA	60	63,700	53
D4	PSI–*g*–poly(NIPAM–*co*–DMA)	1.6 NIPAM/1 DMA	88	78,000	51–52
D5	PSI–*g*–poly(NIPAM–*co*–DMA)	3.2 NIPAM/1 DMA	85	124,000	43
D6	PSI–*g*–poly(NIPAM–*co*–BA)	4 NIPAM/1 BA	85	52,000	–
D7	PSI–*g*–poly(NIPAM–*co*–BA)	7 NIPAM/1 BA	86	107,000	–

diethyl ether, and dried under vacuum. The characteristics of the synthesized polymers are presented in Table 1.

Characterization

The polymers were characterized by ^{1}H NMR, fluorescence spectroscopy, DSC, dynamic light scattering (DLS) and rheology coupled with SALS (small angle light scattering). The ^{1}H NMR spectra were recorded on a Bruker 400 MHz apparatus. DSC curves were recorded on a Mettler DSC12E calorimeter with a heating/cooling rate of 10 K/min.

The classical method using pyrene fluorescence spectroscopy was applied to evaluate the amphiphilic polysiloxanes' aggregation capacity [36]. The critical concentration of aggregation (CCA) value was calculated using the first (named I_1) and the third (named I_3) absorption peaks corresponding to the fluorescence emission spectrum of pyrene. In aqueous solution, the I_1/I_3 ratio value corresponding to the free pyrene in water (not incorporated in the micelles) is situated around 1.70–1.75 (at room temperature, 25 °C). For concentrations lower than 10^{-2} g/L, no aggregation process was evidenced, the I_1/I_3 ratio being around 1.7 [1]. For fluorescence measurements a Rf-5301PC Shimadzu spectrofluorometer was used.

The aggregate' morphology was studied using DLS and Rheo-SALS methods. The DLS experiments were performed on a Zetasizer Nano ZS (Malvern Instruments, Southborough, MA) equipped with a He–Ne laser source ($\lambda = 633$ nm), the autocorrelation function being automatically calculated.

Rheological measurements were carried out using a rheometer Physica MCR 501 (Anton Paar, Austria) with a Peltier device for the temperature control. Parallel plate geometry with serrated plates to avoid slippage was used. The upper plate from stainless still was 50 mm in diameter. A solvent trap was used in all rheological tests to diminish the solvent evaporation.

Combined rheological and SALS (Rheo-SALS) experiments during shear were performed using the Physica MCR 501 rheometer, equipped with a specially designed parallel plate–plate configuration (the diameter of the plate is 43 mm) in glass. The instrumentation for the Rheo-SALS experiments was purchased from Anton Paar Austria. In all measurements a 10 mW diode laser operating at a wavelength of 658 nm was used as the light source, and a polarizer was placed in front of the laser and an analyzer below the sample, making both polarized (polarizer and analyzer parallel) and depolarized (polarizer and analyzer perpendicular) experiments possible. Utilizing a prism, the laser beam was deflected and passed through the sample placed between the transparent parallel plates. The sample was applied onto the lower plate. The distance between the plates is small (0.5 or 1.0 mm), so the effect of multiple scattering was reduced when the sample became turbid at elevated temperatures. The two-dimensional scattering patterns formed on the screen were captured using a CCD camera (driver LuCam V. 4.5), whose plane was parallel to that of the screen. A Lumenera (VGA) CCD camera (Lumenera Corporation, Ottawa, Canada) with a Pentax lens was utilized, and the scattered images were stored on a computer using the StreamPix (NorPix, Montreal, Quebec, Canada) application software, which enables a real-time digitalization of the images. The images were acquired via the CCD camera with an exposure time of 200 ms. Subsequently, the pictures were analyzed using the SALS software program (version 1.1). The software package contains an analyzing program developed at the University of Leuven (Belgium), which allows analyzing the images of the scattered light [37–39].

Results and discussion

The polymers' molecular weights (M_n) were calculated using ^{1}H NMR spectra, by taking into account the substitution degree (the starting polysiloxane containing

chlorobenzyl groups has for all the samples a molecular weight value $M_n = 4{,}800$–$5{,}000$). Except sample D3 with a grafting degree of only 60 %, for all other samples the value is higher than 85 %.

In Fig. 1 the ^{1}H NMR spectra corresponding to the polysiloxane grafted with PNIPAM (a) and with PDMA (b) are presented. The signal corresponding to the methylenic groups of NIPAM appears at 1.25 ppm and the specific signal for methyl groups in DMA is present at 2.9 ppm. In both spectra the signal corresponding to the methyl groups from polysiloxane (reference signal for polysiloxane structural unit) can be observed at 0.1 ppm. Another characteristic signals are: at 4.0 ppm (Fig. 1a) –CH-group from NIPAM; 1.5–2.5 ppm aliphatic region corresponding to the PNIPAM and PDMA main-chain; 7.1 ppm aromatic rings from polysiloxane.

The glass transition temperatures have been evidenced by DSC analysis (Table 2). Dynamic scanning calorimetric studies have been carried out on 3–5 mg samples with a Mettler Toledo DSC-1 Star System at a nitrogen flow rate of 150 mL/min. For all samples two heating and one cooling cycles have been performed between −40 and 140 °C as a function of the thermal stability of each system. Since the first heating scan is influenced by the sample's "history", only the curves corresponding to the second heating scan are presented in Fig. 2.

PNIPAM, PDMA and the other side chains bonding on the polysiloxane backbone lead to the increase of the glass transition temperature from −40 °C (for the starting polysiloxane) to more than 70 °C for samples D2, D3, D5, and D6 and even above 100 °C for sample D7. Obviously long graft-chains diminished the influence of the PSI backbone to the overall value of the glass transition temperature.

Amphiphilic graft or block polymers have the ability to generate micelles in aqueous solutions [40]. The polymers synthesized in this study are amphiphilic graft polymers bearing hydrophilic side chains on a hydrophobic polysiloxanic backbone. Moreover these systems have stimuli responsive entities in their structure. The amphiphilic polymers with thermo-sensitive elements are of particular interest because they can self-assemble into various micro and nanostructures, suitable for various biomedical applications [41]. Therefore, the next step of the study was to verify if the amphiphilic graft polysiloxanes are capable to generate micelles and to evaluate their critical concentration of aggregation (CCA) values. The CCA values were estimated as the first inflexion point from the curves that represent the plot of the I_1/I_3 ratio as a function of the polymer concentration (Fig. 3) and they range between 0.043 and 0.15 g/L. Micelles formed from the graft polysiloxanes are composed of hydrophobic polysiloxane core and a thermo-sensitive hydrophilic shell.

In agreement with the literature data published by Matyjaszewski group we supposed that increasing temperature, PNIPAM in the shell dehydrate and more inter- and intra-molecular H bonds are formed, the core hydrophobicity increases and micelles collapse. Cooling the system the H bonds are broken and the micelles expand. This particular behavior is important in biomedical applications when guest molecules can be encapsulated noncovalently, and their release can be controlled by external stimuli. The aggregation/disaggregation phenomena can be tailored throughout the polymers architecture and the hydrophobic/hydrophilic balance in the macromolecule.

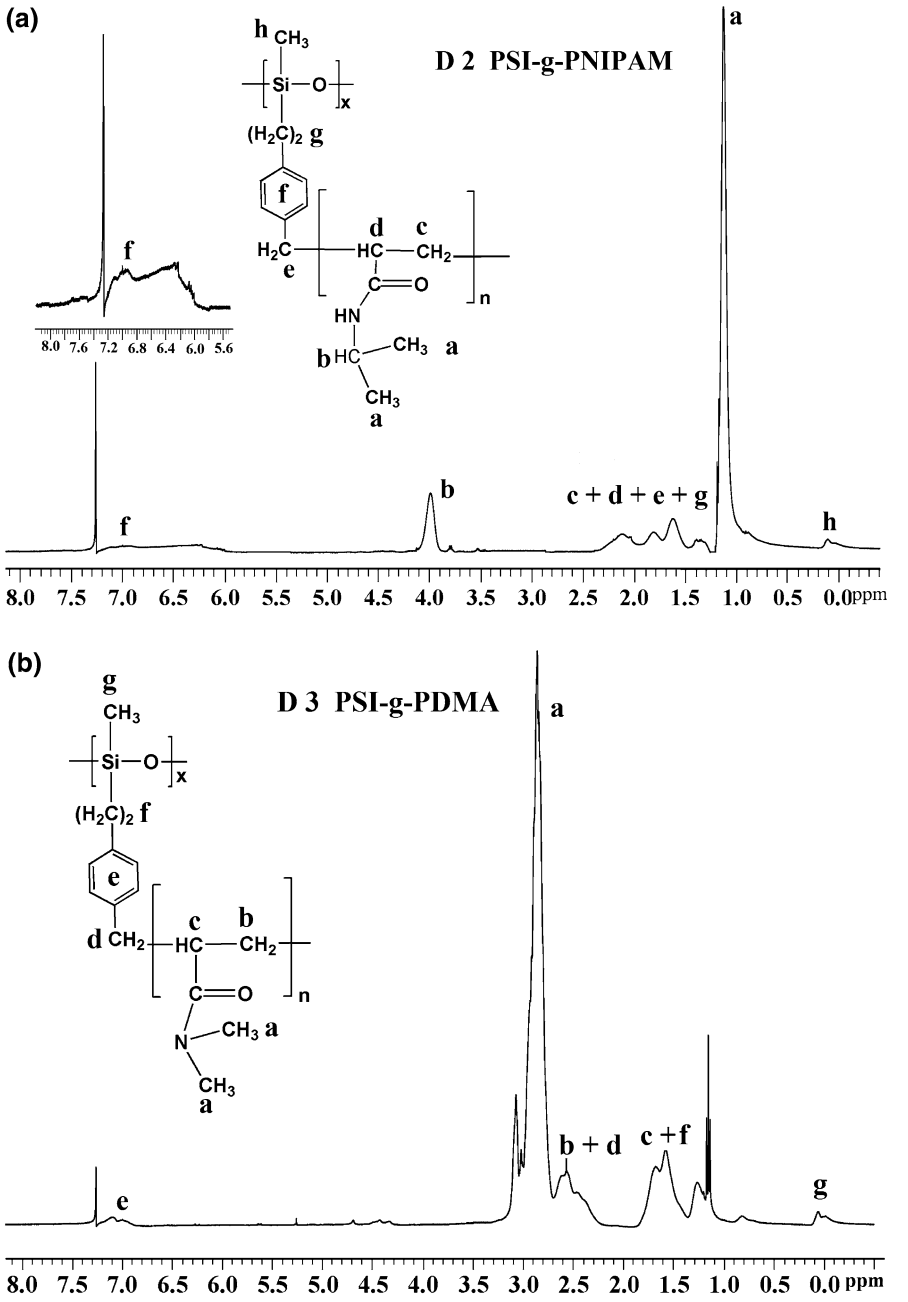

Fig. 1 ^{1}H NMR spectra of samples D2 (**a**) and D3 (**b**)

Table 2 Glass transition temperatures of the synthesized polymers

SAMPLE	D1	D2	D3	D4	D5	D6	D7
T_g, °C	117	89	88	62	87	73	103

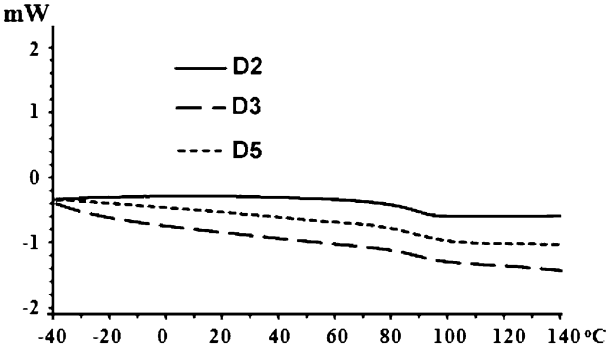

Fig. 2 DSC curves of PNIPAM (D2), PDMA (D3) and PNIPAM–*co*–PDMA (D5) graft linear polysiloxane

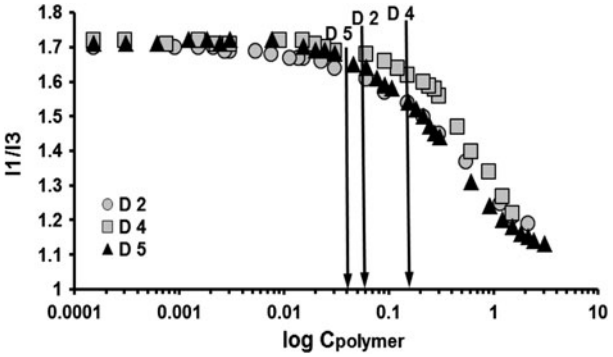

Fig. 3 Plot of the I_1/I_3 ratio as a function of the graft polysiloxane concentration corresponding to the samples D2, D4, and D5

Rheological behavior of graft polysiloxanes

Rheological oscillatory tests are widely used to characterize and quantify the macroscopic behavior of multiphase viscoelastic polymeric systems as well as their internal structure. Typical measured parameters are the storage modulus G' (a measure of the *deformation energy stored* by the sample during the shear process, representing the *elastic behavior* of the material), loss modulus G'' (a measure of the *deformation energy used* by the sample during the shear process, representing the *viscous behavior* of the material), phase angle δ, damping, or loss factor: tan $\delta = G''/G'$ (revealing *the ratio of the viscous and the elastic portion* of the viscoelastic deformation behavior) and complex viscosity $|\eta^*|$ [42–44]. Dynamic

oscillatory testing is a recognized way to reveal interesting data about microstructure of the materials and to correlate them with the macroscopic behavior.

Comparative rheological studies have been carried out on a series of aqueous solutions of the synthesized polymers of different concentrations (between 0.1 and 5 mg/mL).

Three types of rheological measurements were carried out: amplitude sweep; temperature sweep (oscillation); rotational temperature tests. During all rheological experiments a solvent trap was used to minimize the evaporation.

The amplitude sweep is generally used to determine the linear-viscoelastic range (LVR). Here, the oscillation frequency was kept constant ($\omega = 10$ rad/s), while the oscillation amplitude (γ) was varied (between 0.01 and 100 %). All experiments were carried out at 25 °C. Tests at different frequencies (between 0.5 and 30 rad/s) were also performed to check the influence of frequency on the LVR. No significant influence of frequency on LVR was found so for all subsequent tests a deformation of 5 % was selected (placed within the LVR for all samples). Little influence of solution concentration on LVR was noticed.

A temperature sweep was carried out for all samples to evidence phase transitions induced by temperature and the thermo-associative phenomena. In the temperature tests constant frequency ($f = 1$ Hz) and constant amplitude of deformation (5 % within the LVR limits for each sample) were presetted, and the temperature was varied between 5 and 80 °C (with a heating rate of 0.5 °C/min).

Figure 4 presents the temperature test for a 3 mg/mL solution of PSI–*g*–poly(NIPAM–*co*–DMA) (D4) in terms of dynamic moduli (G' and G'') and complex viscosity ($|\eta^*|$). As supposed conformational changes of macromolecules were observed when temperature was increased. PNIPAM and PDMA have LCST values of approximately 32 and above 100 °C [45, 46], respectively, and graft polysiloxanes with side chains of these polymers or copolymers of NIPAM and DMA are

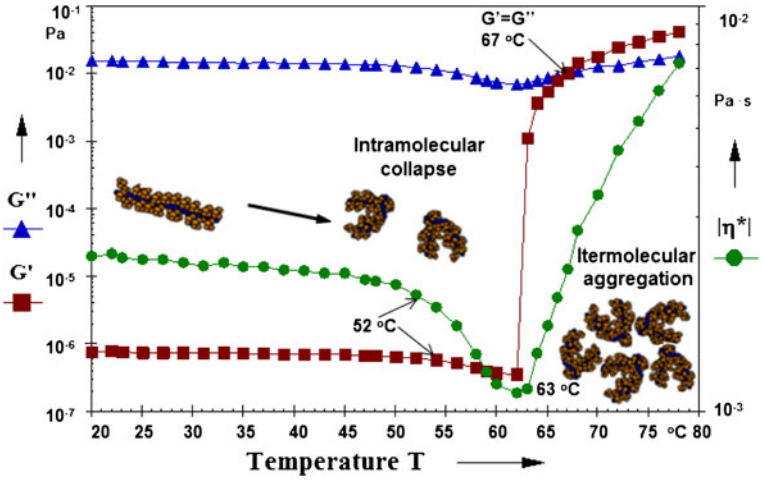

Fig. 4 Temperature sweep for a 3 mg/mL solution of PSI–*g*–poly(NIPAM–*co*–DMA) (D4) and suggested mechanism of association

expected to have LCST values in between. We supposed rheological tests to give an insight into the association/dissociation phenomena occurring in systems based on thermo-sensitive polymers with temperature. For low temperatures a specific liquid-like viscoelastic behavior is characteristic with $G'' > G'$. The structure is stable and between 5 and 51 °C the dynamic moduli are almost parallel. Here the polymer is under its LCST and adopts an extended conformation probably due to hydrogen bonding between the amide groups of the copolymer and water molecules. Continuously increasing the temperature, a slight decrease of the moduli, and a more evident decrease in the complex viscosity appears over 51 °C as a consequence of the dehydration of individual chains and beginning of the intramolecular collapse which facilitates the sliding of the macromolecules [45]. Thereafter, a sharp decrease of the complex viscosity is noticed together with the decrease in both moduli.

At 63 °C the minimum on the G'' and $|\eta^*|$ curves is reached while G' sharply increases. Correlating with DLS results we supposed the first point where an evident change (decrease or increase depending on the mechanism involved) in the rheological parameter appears as an indication for the LCST of the polymer. As discussed later on this assumption is in good correlation both with DLS data and visual observations, the solutions turning from clear to turbid. Over 63 °C both G' and $|\eta^*|$ increase until 67 °C where the cross-over point of the two dynamic moduli is reached. For higher temperatures a solid-like (gel) structure is characteristic specific to the intermolecular aggregation of the macromolecules and jamming of the bigger aggregates. We supposed for this polymer both intramolecular collapse and then intermolecular aggregation could be rheologically evidenced.

Somewhat different behavior was observed for PSI–*g*–PNIPAM (D2) for different solution concentrations (Fig. 5). For PSI–*g*–PNIPAM the first increase in the rheological parameters appears around 31 °C (detail in Fig. 5). At this

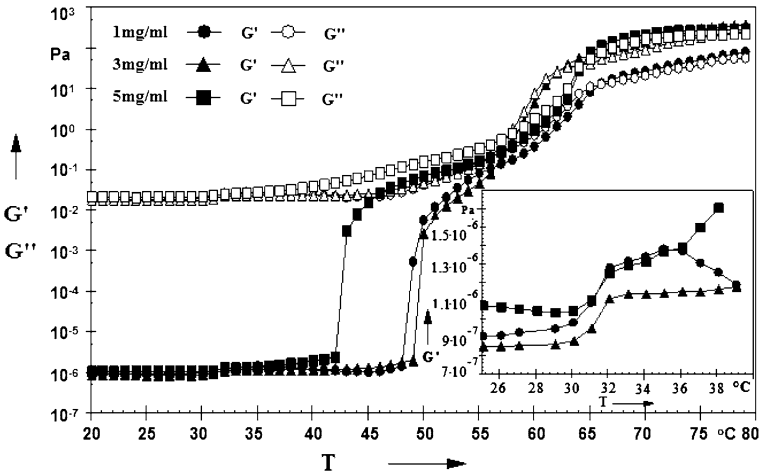

Fig. 5 Temperature sweep for solutions of PSI–*g*–PNIPAM (D2) of different concentrations (detail—cross-over point of G' and G'')

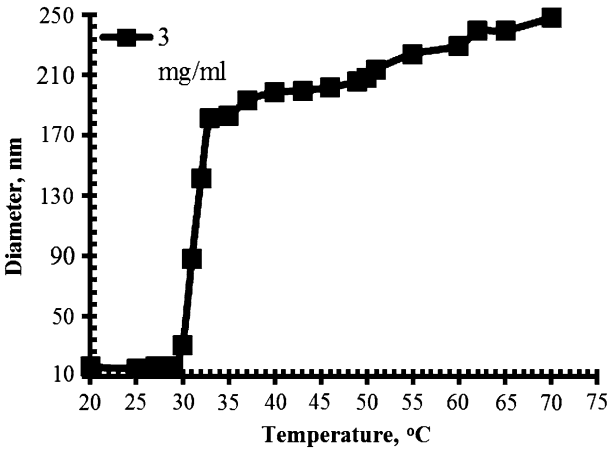

Fig. 6 Apparent hydrodynamic average diameters as a function of temperature for a 3 mg/mL solution of PSI–*g*–PNIPAM (D2)

temperature the solutions change visually from clear to turbid. Also from the DLS measurements the beginning of the increase in the aggregates dimensions is noticed at this temperature. So we supposed the LCST for this polymer to be around 32 °C. Then the intermolecular aggregation develops and the dimensions of the aggregates continuously increase as could be noticed both from rheological and DLS data (Fig. 6). Increasing solution concentration from 1 to 5 mg/mL has not noticeable influence on the LCST value, but a difference of almost 10 °C is observed for the temperature of intermolecular aggregation. As stated in the literature [45] the concentration could have an important influence on the aggregation processes due to the decrease in the distance between the macromolecular branches.

The presence of hydrophilic DMA units in the side chains shifts the LCST to higher temperatures (see Figs. 4, 7). Also the structure of the side chains changes the shape of G' and G'' curves due to different ways and rates of the intermolecular aggregation process. The formation of the intermolecular aggregates is a one or two step process depending on the structure and architecture of the branches.

The systems based on PSI–*g*–poly(NIPAM–*co*–BA) (samples D6 and D7) have a reduced solubility in water and the rheological results were not conclusive.

Rheological data describe the macroscopic behavior but more interesting is to gain an insight in the sample's structure and to correlate the structure with the rheological properties. The microstructure of a sample determines the macroscopic behavior and as a consequence the rheological properties. The combination of a SALS equipment (Physica Rheo-SALS) and a Physica rheometer permits, by the integration of the optical method, a direct correlation between the rheological behavior and the microstructure of the sample [47]. The aim is to examine how the interplay between intermolecular and intramolecular cross-liking/associations under the influence of shear is affected by hydrophobic/hydrophilic modification of the polymer and the polymer architecture. For this purpose we employed Rheo-SALS method to simultaneously monitor rheological and structural modifications. In light

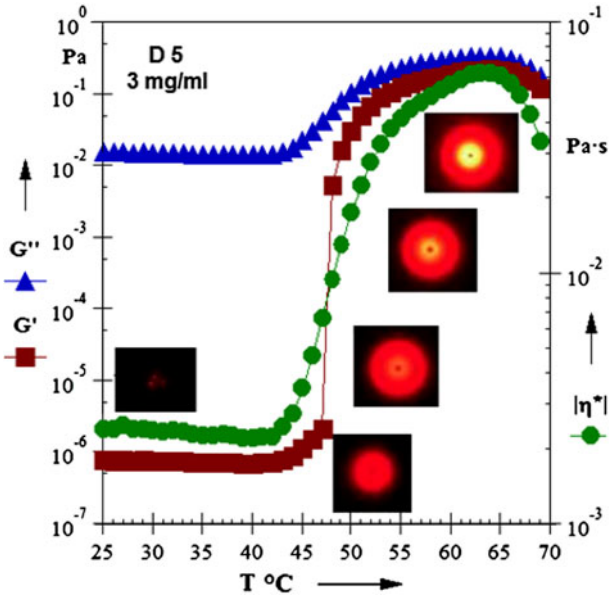

Fig. 7 Temperature sweep and Rheo-SALS images for a solution of PSI–*g*–poly(NIPAM–*co*–DMA) (D5)

scattering the angular distribution of the scattered light, which is induced by an incoming primary laser beam is measured and analyzed with respect to angle and intensity. Under certain assumptions structural information can be obtained from the scattered light intensity distribution.

Figure 7 presents the temperature sweep and the corresponding Rheo-SALS images for a PSI–*g*–poly(NIPAM–*co*–DMA) (sample D5) 3 mg/mL solution. As for sample D2 the intramolecular collapse could not be clearly evidenced but the dimensional increase of aggregates after LCST due to the intermolecular aggregation is clear on the rheological curves. Scattered intensity patterns increase with the increase in temperature supporting the assumptions of the proposed mechanism. These observations are also valid for all the analyzed samples.

Moreover the results from the oscillatory temperature tests are confirmed by the rotational temperature tests (Fig. 8). Several viscosity measurements were performed. Here the shear rate was kept constant ($\dot{\gamma} = 20\ s^{-1}$) while the temperature was varied between 20 and 70 °C with a heating rate of 0.5 °C/min (this heating rate was also used in Rheo-SALS experiments). Both the relative viscosity (η) and the shear stress (τ) are decreasing when temperature is increased from 20 to 42 °C.

Continuously increasing the temperature the intermolecular aggregates are formed, and the viscosity, as well as the shear stress increase. The characteristic temperature for the sharp increase both in viscosity and shear stress is the approximately the same like in the oscillatory temperature tests and Rheo-SALS experiments and corresponds to the visual observation when the aspect of the solution turns from clear to turbid.

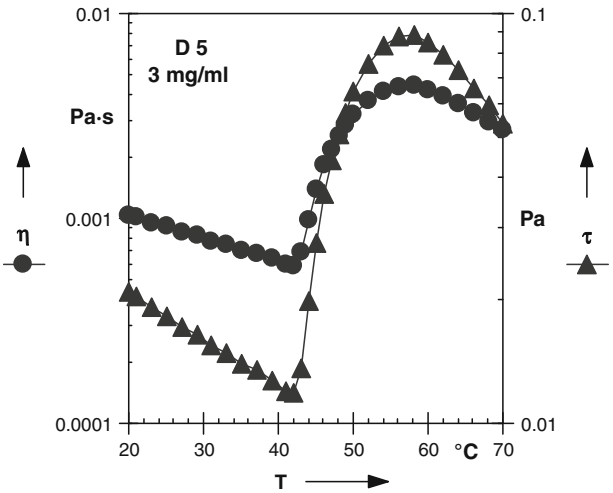

Fig. 8 Temperature dependency of the shear viscosity and shear stress of PSI–*g*–poly(NIPAM–*co*–DMA) (D5) 3 mg/mL solution

Finally we checked the correspondence between the rheologically observed aggregation phenomena and DLS data. Figure 9 presents DLS and Rheo-SALS results for the D1 sample, a 3 mg/mL solution of PNIPAM.

The thermo-sensitive behavior of PNIPAM was intensively studied so the correlation we found was an indication that our assumptions are valid also for the rheological and Rheo-SALS data. The differences in the characteristic temperature between DLS and rheological and Rheo-SALS measurements are very small (maximum 1–2 °C) for all analyzed polymer systems.

As easily can be noticed from all rheological curves and Rheo-SALS results the thermo-sensitive character of the synthesized polymers could be evidenced and a good correlation was found with DLS data. Different mechanisms apply with particular features depending on the nature and architecture of the side chains. As expected, grafting NIPAM on a flexible hydrophobic PSI backbone produces a thermo-sensitive polymer with a LCST close to the characteristic value for PNIPAM. Higher LCST values are characteristic for PSI graft with PDMA or copolymers NIPAM–DMA. Increasing the proportion of NIPAM in the copolymer decreases the LCST value. The solution concentration has noticeably influence on the aggregation process. The collapse of the macromolecular chains in aggregates with compact structure was evidenced for samples D4 and the formation of intermolecular aggregates at temperatures higher than LCST for all water-soluble samples.

Conclusion

Grafting linear PSI with NIPAM, DMA, and copolymers of NIPAM with DMA using SET-LRP technique allows developing polymers characterized by high

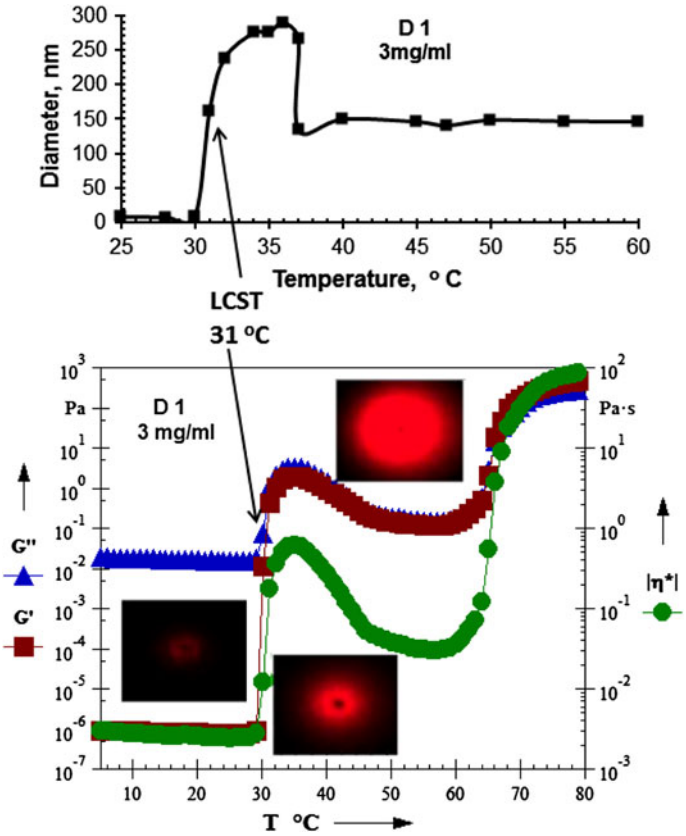

Fig. 9 Temperature sweep and Rheo-SALS images for a solution of 3 mg/mL PNIPAM (D1) correlated with DLS data

flexibility and controlled thermo-sensitivity. The coil to globule transition of copolymer side chains and thus the LCST of the resulted polymers can be tuned by modifying structure of branches and the ratio of the structural units in the statistic copolymers. Different mechanisms involving both intra- and intermolecular aggregation or only one of them can be involved depending on the architecture of the system and the solution concentration. Rheological and Rheo-SALS measurements proved to be useful tools to characterize the macroscopic behavior but also to evidence structural changes below and above the LCST for the analyzed systems. Good correlation was found between rheological, rheo-SALS and DLS data. Samples D2 and D5 are the most promising materials for further biological applications.

Acknowledgments The authors are grateful for the financial support provided by the BRAIN project "Doctoral scholarships as an investment in intelligence", financed by the European Social Found and Romanian Government ANCS Grant 01CEA/2010 BIO-AZO. Rheological and Rheo-SALS measurements were carried out in the Laboratory of Rheology of the Interdisciplinary training and research Platform MATMIP (Cod CNCSIS 69/2006).

References

1. Moleavin I, Grama S, Carlescu I, Scutaru D, Hurduc N (2010) Photosensitive micelles based on polysiloxanes containing azobenzene moieties. Polym Bull 65:69–81. doi:10.1007/s00289-010-0247-4
2. Gil ES, Hudson SM (2004) Stimuli-responsive polymers and their bioconjugates. Prog Polym Sci 29:1173–1222. doi:10.1016/j.progpolymsci.2004.08.003
3. de las Heras Alarcón C, Pennadam P, Alexander C (2005) Stimuli responsive polymers for biomedical applications. Chem Soc Rev 34:276–285. doi:10.1039/B406727D
4. Wong SY, Pelet JM, Putnam D (2007) Polymer systems for gene delivery—past, present, and future. Prog Polym Sci 32:799–837. doi:10.1016/j.progpolymsci.2007.05.007
5. Kumar A, Srivastava A, Galaev IY, Mattiasson B (2007) Smart polymers: physical forms and bioengineering applications. Prog Polym Sci 32:1205–1237. doi:10.1016/j.progpolymsci.2007.05.003
6. Rzaev ZMO, Dincer S, Piskin E (2007) Functional copolymers of *N*-isopropylacrylamide for bioengineering applications. Prog Polym Sci 32:534–595. doi:10.1016/j.progpolymsci.2007.01.006
7. Bajpai AK, Shukla SK, Bhanu S, Kankane S (2008) Responsive polymers in controlled drug delivery. Prog Polym Sci 33:1088–1118. doi:10.1016/j.progpolymsci.2008.07.005
8. Chen T, Ferris R, Zhang J, Ducker R, Zauscher S (2010) Stimulus-responsive polymer brushes on surfaces: transduction mechanisms and applications. Prog Polym Sci 35:94–112. doi:10.1016/j.progpolymsci.2009.11.004
9. Agarwal A, Hess H (2010) Biomolecular motors at the intersection of nanotechnology and polymer science. Prog Polym Sci 35:252–277. doi:10.1016/j.progpolymsci.2009.10.007
10. Medeiros SF, Santosa AM, Fessi H, Elaissari A (2011) Stimuli-responsive magnetic particles for biomedical applications. Int J Pharm 403:139–161. doi:10.1016/j.ijpharm.2010.10.011
11. Cohen Stuart MA, Huck WTS, Genzer J, Müller M, Ober C, Stamm M, Sukhorukov GB, Szleifer I, Tsukruk VV, Urban M, Winnik F, Zauscher S, Luzinov I, Minko S (2010) Emerging applications of stimuli-responsive polymer materials. Nat Mater 9:101–113. doi:10.1038/nmat2614
12. Pagonis K, Bokias G (2007) Temperature- and solvent-sensitive hydrogels based on *N*-isopropylacrylamide and *N,N*-dimethylacrylamide. Polym Bull 58:289–294. doi:10.1007/s00289-006-0617-0
13. Ortega A, Bucio E, Burillo G (2008) New interpenetrating polymer networks of *N*-isopropylacrylamide/*N*-acryloxysuccinimide: synthesis and characterization. Polym Bull 60:515–524. doi:10.1007/s00289-007-0870-x
14. Ramírez-Fuentes YS, Bucio E, Burillo G (2008) Thermo and pH sensitive copolymer based on acrylic acid and *N*-isopropylacrylamide grafted onto polypropylene. Polym Bull 60:79–87. doi:10.1007/s00289-007-0827-0
15. Zhao SP, Li LY, Cao MJ, Xu WL (2011) pH- and thermo-sensitive semi-IPN hydrogels composed of chitosan, *N*-isopropylacrylamide, and poly(ethylene glycol)–*co*–poly(ε-caprolactone) macromer for drug delivery. Polym Bull 66:1075–1087. doi:10.1007/s00289-010-0390-y
16. Yin W, Yang H, Zhang X, Wang Z, Ding Y, Zhang G, Cheng R (2005) Investigation of the self-association behavior of a thermosensitive copolymer with lower critical solubility temperature near human heat by dynamic laser light scattering. J Appl Polym Sci 96:583–588. doi:10.1002/app.21484
17. Schmaljohann D (2006) Thermo- and pH-responsive polymers in drug delivery. Adv Drug Deliv Rev 58:1655–1670. doi:10.1016/j.addr.2006.09.020
18. Dimitrov I, Trzebicka B, Müller AHE, Dworak A, Tsvetanov CB (2007) Thermosensitive water-soluble copolymers with doubly responsive reversibly interacting entities. Prog Polym Sci 32:1275–1343. doi:10.1016/j.progpolymsci.2007.07.001
19. Rosen BM, Percec V (2009) Single-electron transfer and single-electron transfer degenerative chain transfer living radical polymerization. Chem Rev 109:5069–5119. doi:10.1021/cr900024j
20. Ouchi M, Terashima T, Sawamoto M (2009) Transition metal-catalyzed living radical polymerization: toward perfection in catalysis and precision polymer synthesis. Chem Rev 109:4963–5050. doi:10.1021/cr900234b
21. Percec V, Guliashvili T, Ladislaw JS, Wistrand A, Stjerndahl A, Sienkowska MJ, Monteiro MJ, Sahoo S (2006) Ultrafast synthesis of ultrahigh molar mass polymers by metal-catalyzed living radical polymerization of acrylates, methacrylates, and vinyl chloride mediated by SET at 25 °C. J Am Chem Soc 128:14156–14165. doi:10.1021/ja065484z

22. Nguyen NH, Rosen BM, Percec V (2010) SET-LRP of *N,N*-dimethylacrylamide and of *N*-isopropylacrylamide at 25 °C in protic and in dipolar aprotic solvents. J Polym Sci A 48:1752–1763. doi:10.1002/pola.23940
23. Lligadas G, Percec V (2007) Synthesis of perfectly bifunctional polyacrylates by single-electron-transfer living radical polymerization. J Polym Sci A 45:4684–4695. doi:10.1002/pola.22307
24. Lligadas G, Rosen BM, Bell CA, Monteiro MJ, Percec V (2008) Effect of Cu(0) particle size on the kinetics of SET-LRP in DMSO and Cu-mediated radical polymerization in MeCN at 25 °C. Macromolecules 41:8365–8371. doi:10.1021/ma8018365
25. Lligadas G, Rosen BM, Monteiro MJ, Percec V (2008) Solvent choice differentiates SET-LRP and Cu-mediated radical polymerization with non-first-order kinetics. Macromolecules 41:8360–8364. doi:10.1021/ma801774d
26. Lligadas G, Percec V (2008) A comparative analysis of SET-LRP of MA in solvents mediating different degrees of disproportionation of Cu(I)Br. J Polym Sci A 46:6880–6895. doi:10.1002/pola.22998
27. Lligadas G, Ladislaw JS, Guliashvili T, Percec V (2008) Functionally terminated poly(methyl acrylate) by SET-LRP initiated with $CHBr_3$ and CHI_3. J Polym Sci A 46:278–288. doi:10.1002/pola.22379
28. Lligadas G, Percec V (2008) SET-LRP of acrylates in the presence of radical inhibitors. J Polym Sci A 46:3174–3181. doi:10.1002/pola.22635
29. Hatano T, Rosen BM, Percec V (2010) SET-LRP of vinyl chloride initiated with $CHBr_3$ and catalyzed by Cu(0)-wire/TREN in DMSO at 25 °C. J Polym Sci A 48:164–172. doi:10.1002/pola.23774
30. Nguyen NH, Rosen BM, Lligadas G, Percec V (2009) Surface-dependent kinetics of Cu(0)-wire-catalyzed single-electron transfer living radical polymerization of methyl acrylate in DMSO at 25 °C. Macromolecules 42:2379–2386. doi:10.1021/ma8028562
31. Nguyen NH, Rosen BM, Jiang X, Fleischmann S, Percec V (2009) New efficient reaction media for SET-LRP produced from binary mixtures of organic solvents and H_2O. J Polym Sci A 47:5577–5590. doi:10.1002/pola.23665
32. Nguyen NH, Jiang X, Fleischmann S, Rosen BM, Percec V (2009) The effect of ligand on the rate of propagation of Cu(0)-wire catalyzed SET-LRP of MA in DMSO at 25 °C. J Polym Sci A 47: 5629–5638. doi:10.1002/pola.23691
33. Fleischmann S, Rosen BM, Percec V (2010) SET-LRP of acrylates in air. J Polym Sci A 48: 1190–1196. doi:10.1002/pola.23879
34. Jiang X, Fleischmann S, Nguyen NH, Rosen BM, Percec V (2009) The disproportionation of Cu(I)X mediated by ligand and solvent into Cu(0) and $Cu(II)X_2$ and its implications for SET-LRP. J Polym Sci A 47:5591–5605. doi:10.1002/pola.23690
35. Kazmierski XK, Hurduc N, Sauvet G, Chojnowski J (2004) Polysiloxanes with chlorobenzyl groups as precursors of new organic-silicone materials. J Polym Sci A 42:1682–1692. doi:10.1002/pola.11066
36. Hurduc N, Enea R, Rezmerita AM, Moleavin I, Cristea M, Scutaru D (2008) Modified azo-polysiloxanes for complex photo-sensible supramolecular systems. In: Ganachaud F, Boileau S, Boury B (eds) Silicon based polymers. Springer, Berlin, pp 65–84. doi:10.1007/978-1-4020-8528-4_6
37. Heyer P (2004) Identification of flow and structure properties by combining small angle light scattering and rheology. Application Note Physica Rheometers, Anton Paar Germany anpo04011e_sals_b.doc
38. Zhu K, Jin H, Kjøniksen A-L, Nyström B (2007) Anomalous transition in aqueous solutions of a thermoresponsive amphiphilic diblock copolymer. J Phys Chem B 111:10862–10870. doi:10.1021/jp074163m
39. Liu Z, Maleki A, Zhu K, Kjøniksen A-L, Nyström B (2008) Intramolecular and intermolecular association during chemical cross-linking of dilute solutions of different polysaccharides under the influence of shear flow. J Phys Chem B 112:1082–1089. doi:10.1021/jp076497h
40. Pinteala M, Epure V, Harabagiu V, Simionescu BC, Schlick S (2004) Concentration- and pH-dependent conformational changes and aggregation of block copolymers of poly(methacrylic acid) and poly(dimethylsiloxane) in aqueous media, based on fluorescence spectra of pyrene and potentiometry. Macromolecules 37:4623–4634. doi:10.1021/ma0496697
41. Ren Y, Jiang X, Yin G, Yin J (2010) Multistimuli responsive amphiphilic graft poly(ether amine): synthesis, characterization, and self-assembly in aqueous solution. J Polym Sci A 48:327–335. doi:10.1002/pola.23788
42. Barnes HA (2000) Handbook of elementary rheology. University of Wales: Institute of Non-Newtonian Fluid Mechanics, Aberystwyth
43. Mezger TG, The Rheology Handbook, ed. Edition n. Hannover: Vincentz Network GmbH; 2006
44. Ibanescu C, Danu M, Nanu A, Lungu M, Simionescu BC (2010) Stability of disperse systems estimated using rheological oscillatory shear tests. Rev Roum Chim 55(11–12):933–940

45. Pietrasik J, Sumerlin BS, Lee RY, Matyjaszewski K (2007) Solution behavior of temperature-responsive molecular brushes prepared by ATRP. Macromol Chem Phys 208:30–36. doi:10.1002/macp.200600442
46. Fischer F, Zufferey D, Tahoces R (2011) Lower critical solution temperature in superheated water: the highest in the poly(*N,N*-dialkylacrylamide) series. Polym Int 60:1259–1262. doi:10.1002/pi.3071
47. Lauger J, Heyer P, Pfeifer G (2004) A new integrated Rheo small angle light scattering (Rheo-SALS) device. Anu Trans Nordic Rheol Soc 12:137–140